MoS_2/Quantum Dot Hybrid Photodetectors on Flexible Substrates

Ozan Yakar[1,2], Burkay Uzlu[1,2], Daniel S. Schneider[1,2], Annika Grundmann[3], Sören Becker[4], Jan S. Niehaus[4], Hendrik Schlicke[4], Michael Heuken[3, 5], Holger Kalisch[3], Andrei Vescan[3], Zhenxing Wang[1,*], Max C. Lemme[1,2,*]

[1] *AMO GmbH, Advanced Microelectronic Center Aachen (AMICA), 52074 Aachen, Germany*
[2]*Chair of Electronic Devices, RWTH Aachen University, Otto-Blumenthal-Str. 25, 52074 Aachen, Germany*
[3]*Compound Semiconductor Technology, RWTH Aachen, Sommerfeldstraße 18, 52074 Aachen*
[4]*Fraunhofer Center for Applied Nanotechnology CAN, Grindelallee 117, 20146 Hamburg, Germany*
[5]*AIXTRON SE; Dornkaulstraße 4, 52134, Herzogenrath, Germany*
[*]*Email: wang@amo.de; max.lemme@eld.rwth-aachen.de / Phone: (+49) 241-8867-200*

Introduction: MoS_2 is a semiconducting transition-metal dichalcogenide and an attractive candidate for optoelectronics and flexible electronics due to its strong excitonic interactions, low dark current (I_{Dark}) and high mechanical strength. Photodetectors (PDs) based on MoS_2 have been demonstrated with high responsivities and low I_{Dark} [1-3]. However, long response times, often in the range of several seconds, severely limit their use for imaging applications. Hybrid structures made of MoS_2 and colloidal quantum dots (CQDs) have been shown to improve the response times down to the ms range [4]. These devices were made from exfoliated materials and on rigid substrate. Here, we present hybrid MoS_2/CQDs based PDs with high performance using a scalable fabrication approach on flexible polyimide (PI) substrates with metalorganic vapor phase epitaxy (MOVPE) grown MoS_2. Our MoS_2/CQDs PDs show fast response times in the ms range and withstand mechanical strain, which provides evidence that our scalable process on PI substrates is a promising approach towards flexible optoelectronics, e.g. wearable sensors or healthcare systems.

Device Fabrication: Flexible substrates were prepared by spin coating liquid PI on silicon (Si) substrates, which was used as a support layer through the fabrication. After coating, the samples were cured at 350 °C, resulting in ~ 8 µm thick PI films. Local back gates were defined by lithography, sputter deposition of 30/10 nm Al/Ti and a lift-off process. 40 nm of Al_2O_3 was deposited as a gate dielectric using atomic layer deposition (ALD) and fluorine based reactive ion etching (RIE) was used to open vias in the Al_2O_3 to access the gate electrode contacts. Few-layer MoS_2 films grown by MOVPE on sapphire substrates [5] were transferred by a PMMA assisted transfer method. MoS_2 channels with lengths/widths of 4/25 µm were defined using contact lithography and patterned using fluorine based RIE. 30/50 nm Ni/Al contacts were sputtered to provide edge contacts to the MoS_2 channels. The PbS CQDs were spin coated on the PDs in octane solution, resulting in a thickness of ~ 100 nm. The devices were encapsulated by 100 nm of electron beam evaporated Al_2O_3 (optical micrograph and device schematic in Fig. 1).

Results: An absorption spectrum of the CQDs is shown in Fig. 2. The MoS_2/CQDs PDs were first characterized in the dark and with optical power densities from 3.5 W/m² to 19 W/m² under ambient conditions. An LED with a wavelength of 630 nm with a spectral full width at half maximum of 10 nm was used as an illumination source. Transfer characteristics show that the MoS_2 is n-type and upon illumination, the channel conductance increases (Fig. 3). This indicates that the photogenerated electrons are transferred to the MoS_2 channel while the photogenerated holes remain trapped in the CQDs layer [4]. Output characteristics of the PDs were measured under dark and illuminated conditions with the phototransistor in the on- (V_G = 10 V) and off-state (V_G = -10 V), respectively (Fig. 4). Gating allows the tuning of I_{Dark}, which is reduced by a factor of ~ 100 when applying a V_G = -10 V. Fig. 5 shows the calculated responsivity as a function of source-drain voltage (V_{DS}) for different V_G. The responsivity in the off-state reaches up to 10^2 A/W for V_{DS} = 3 V while I_{Dark} is kept to ~ 10^{-9} A. In the on-state, the responsivity values reach up to 10^4 A/W at an expense of an increased I_{Dark} of ~ 10^{-6} A. High specific detectivities (D*), ~ 10^{12} Jones and ~ 10^{13} Jones in the off- and on-states are achieved, respectively (Fig. 6). Transient characteristics were investigated by measuring the time delay between the illumination and the PD responses (Fig. 7). The rise time of our MoS_2/CQDs PDs is ~40 ms, a value that is limited by our measurement setup and sufficient for imaging applications [6]. After the PI was peeled off from Si substrate, the mechanical durability of the PDs was tested by measuring the I_{Dark} and photocurrent after up to 500 bending cycles with a radius of 6.4 mm. No significant degradation of the PD performance was observed (Fig. 8-9).

Conclusions: We have demonstrated hybrid MoS_2/CQDs photodetectors with MOVPE-grown MoS_2 with comparable performance to the state-of-the-art in literature from exfoliated materials (Table 1). Our fabrication approach is scalable to wafer scale, and the performance has been achieved on flexible substrates. The results indicate the potential of MoS_2/CQDs PDs for applications in flexible electronics.

Acknowledgements: European Union's Horizon 2020 research and innovation programme under grant agreements GrapheneCore3 (881603), MISEL (101016734), 2Exciting (956813), QUEFORMAL (829035); DFG: GLECS2 (273177991), 2D-MOCVD (VE 597/5-1), MOSTFLEX (407080863), ULTIMOS2 (LE 2440/8-1)

[1] D. Schneider, *et al. ACS Photonics*, 7.6, 1388, (2020).
[2] J. Marin, *et al. npj 2D Mater Appl.*, 3, 1-6, (2019).
[3] Y. Lim, *et al. Adv. Materials*, 28(25), 5025. (2016).
[4] O. Özdemir, *et al., ACS Photonics*, 6, 2381, (2019).
[5] M. Marx, *et al. J. of Crystal Growth*, 464, 100, (2017).
[6] G. Konstantatos, *et al., Nature Nano*, 7, 363 (2012).

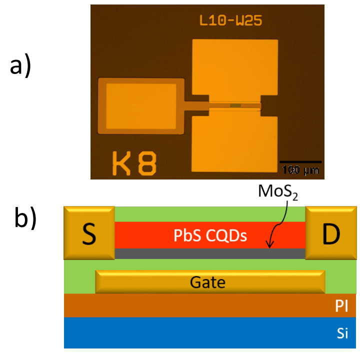

Fig. 1: a) Microscope image and b) schematic of the MoS_2/CQD hybrid photodetector. Green bar represents Al_2O_3.

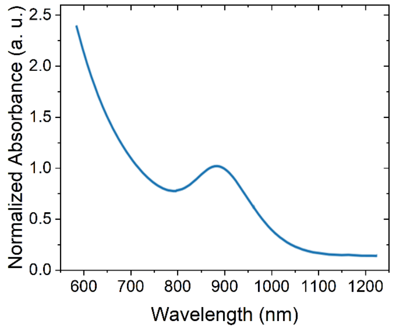

Fig. 2: Absorbance spectrum of the PbS CQDs in octane solution.

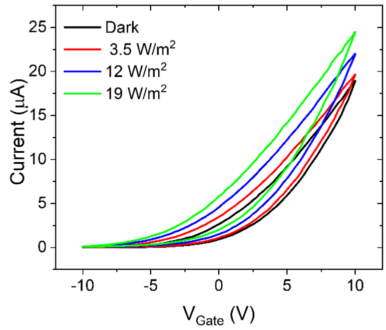

Fig. 3: I/V characteristics of the MoS_2/CQD based photodetector in dark and under illumination at λ= 630 nm for V_{DS}= 3 V.

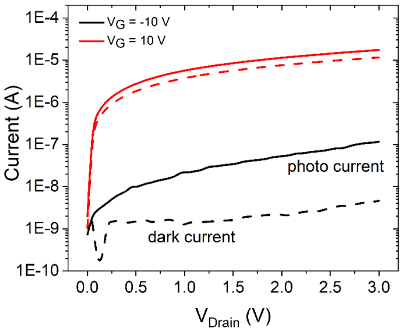

Fig. 4: Photocurrent and the I_{Dark} of the photodetector for V_G= 10 V (on-state) and V_G = -10 V (off-state) λ = 630 nm, P_{LED} = 3.5 W/m²

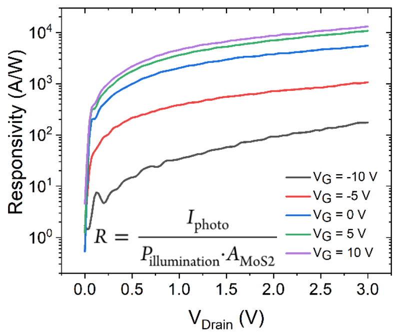

Fig. 5: Responsivity as a function of V_{DS} for varying gate voltages. λ = 630 nm, P_{LED}= 3.5 W/m².

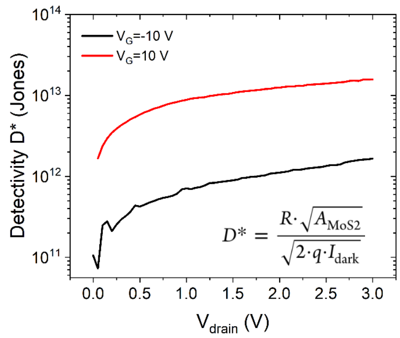

Fig. 6: Specific detectivity of the MoS_2/CQD photodetector as a function of drain voltage.

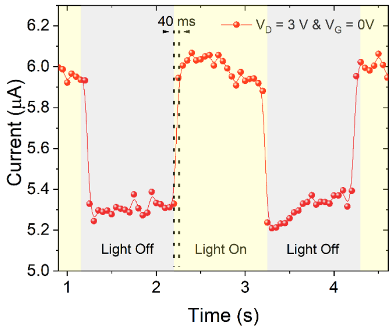

Fig. 7: Transient characteristics of a MoS_2/CQD photodetector.

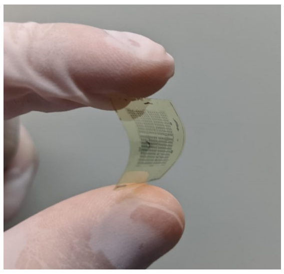

Fig. 8: Photograph of an array of MoS_2/CQD photodetectors on polyimide substrate.

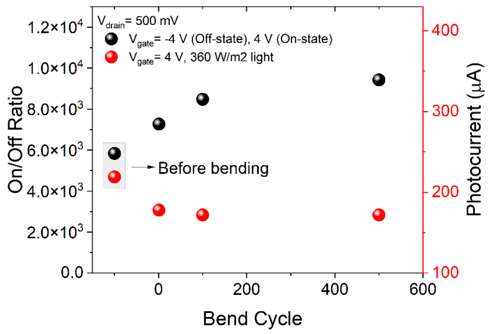

Fig. 9: On/off ratio in dark and photocurrent of MoS_2 photodetector, measured before bending and after each bending cycle (1, 100, 500) with a bending radius of 6.4 mm.

Device Type	Responsivity (A/W)	Resp. Time	I_{dark} (A)	Device Type	Responsivity (A/W)	Resp. Time	I_{dark} (A)
Si[6]	0.5	1-500 ns	~ 10^{-10}	**MoS_2[1]**	~ 10^2-10^3	~500 ms	~ 10^{-10}-10^{-4}
GFET/ CQD[6,*]	~ 10^7	~ 30 ms	~ 10^{-5}	**MoS_2/ CQD[4,*]**	~ 10^0-10^2	~ 30 ms	~ 10^{-10}-10^{-6}
WS_2/ CQD[4,*]	~ 10^2-10^3	~ 200 ms	~ 10^{-8}-10^{-6}	**This Work**	~ 10^2-10^4	~ 40 ms	~ 10^{-9}-10^{-5}

Table 1: Comparison of the state-of-the-art photodetectors with MoS_2/CQD photodetectors in terms of the responsivity, response time and dark current. * *exfoliated materials were used.*